

Clairvoyant: Predictive SJF Scheduling to Mitigate Head-of-Line Blocking in Serial LLM Backends

Aravind Sundaresan*
Independent Researcher
aravindsharma20@gmail.com

Abstract

Serial LLM inference backends—such as Ollama—process requests one at a time under FCFS admission, causing Head-of-Line Blocking (HOLB) under mixed workloads at high utilisation: short factual queries can be delayed by minutes behind long generation jobs. While cloud-scale deployments mitigate HOLB via continuous batching (vLLM, Orca), these solutions require tens of GB of VRAM for concurrent KV-caches—*infeasible* for memory-constrained edge and local deployments that rely on serial request dispatch. We present **Clairvoyant**, a drop-in sidecar proxy for any serial OpenAI-compatible backend (e.g., Ollama, llama.cpp). **Clairvoyant** predicts response length from 19 lightweight lexical features via an ONNX-exported XGBoost classifier, achieving 0.029 ms per-request latency (four orders of magnitude below typical generation time). Because admission scheduling depends on relative ordering rather than exact prediction, the system optimises ranking fidelity, achieving 62–96% in-distribution and 52–66% cross-distribution accuracy across natural conversation datasets. We find that curated instruction datasets are degenerate training sources for length prediction: GPT-imposed brevity constraints reduce Long-class representation to under 0.02% of examples, making natural conversation logs the only viable training source. End-to-end GPU benchmarks on an RTX 4090 show 70–76% P50 latency reduction for short requests under maximum queue pressure (100 concurrent requests, $n = 250$ per cell) and 17% under steady-state Poisson arrivals ($\rho = 0.74$). **Clairvoyant** is open-source and requires no modifications to the inference backend.

1 Introduction

Serial LLM inference backends process requests sequentially under First-Come-First-Served (FCFS) admission. Output generation lengths in mixed workloads span two orders of magnitude: short factual queries require < 10 tokens (~ 2 s), while complex generation tasks exceed 1000 tokens (> 60 s). In single-concurrent-request deployments—edge AI, local enterprise servers, and resource-constrained environments running quantized Small Language Models—this variance causes Head-of-Line Blocking (HOLB): a short request arriving behind a long-generation job waits the full duration of that job before execution begins.

While cloud-scale deployments mitigate HOLB via continuous batching (vLLM [10], Orca [20]), these solutions require, even for 8B-class models at modest concurrency, tens of GB of VRAM for KV-cache maintenance alone [10]—beyond the capacity of consumer and edge hardware. Backends such as Ollama and llama.cpp rely on serial request dispatch by default; no scheduling layer exists between the API endpoint and the inference engine, leaving FCFS as the only admission policy. In local mixed-workload tests on an Apple M1 (Ollama, Gemma3:4b), **Clairvoyant** achieves correct SJF dispatch ordering in end-to-end burst tests, with short requests completing before all long requests under representative mixed workloads (Section 5).

Shortest-Job-First (SJF) scheduling reduces mean waiting time relative to FCFS; the preemptive variant (SRPT) is optimal in the M/G/1 queue [14], but preemption is infeasible for autoregressive generation. We

*Feedback welcome: aravindsharma20@gmail.com

therefore adopt non-preemptive SJF as the admission policy. For LLMs, output length is unknown until generation completes. Prior approaches address this via auxiliary proxy models—fine-tuned BERT-base [13] or DistilBERT [7]—that introduce additional memory footprint, separate inference overhead, and deployment complexity [19].

We present **Clairvoyant**, a drop-in sidecar proxy for serial OpenAI-compatible backends (e.g., Ollama, llama.cpp) that implements non-preemptive SJF admission, mitigating HOLB with 0.029 ms per-request overhead. **Clairvoyant** extracts 19 lightweight lexical features from each incoming request and derives a ranking signal using an XGBoost model exported to ONNX—requiring no prompt embedding and no forward pass through the target model. On Apple M1 (Ollama, Gemma3:4b), **Clairvoyant** achieves correct SJF dispatch ordering in a controlled end-to-end dispatch test ($n = 8$, 4 Short + 4 Long; dispatch-logic validation only—Section 5); queue-level latency statistics derive from $n = 250$ -per-cell GPU benchmarks.

We design, implement, and evaluate **Clairvoyant** across three regimes: (1) offline ranking fidelity on held-out dataset splits, (2) end-to-end GPU latency under burst and steady-state workloads, and (3) starvation-timeout sensitivity via discrete-event simulation calibrated to measured service times. Our evaluation yields five contributions:

1. **Dataset Bias in Length Prediction.** Curated instruction datasets (Alpaca 52K, CodeAlpaca 20K) contain $< 0.02\%$ Long-class examples due to GPT-imposed brevity constraints (Table 2), rendering them degenerate training sources for any length-predictive scheduler. Only natural conversation logs provide sufficient Long-class diversity.
2. **Lexical Sufficiency for Queue Ordering.** We demonstrate that embeddings are unnecessary for admission scheduling in this regime. Nineteen lexical features achieve 62–96% in-distribution ranking accuracy across three natural conversation datasets (Table 5), with predictor latency (0.029 ms) compatible with serial edge deployment (Section 3.3).
3. **Zero-Modification Admission Architecture.** **Clairvoyant** operates as a transparent sidecar proxy for OpenAI-compatible backends, requiring no changes to the inference engine, no model fine-tuning, and no forward pass through the target LLM (Figure 2).
4. **Empirical Queue Management.** We implement an SJF min-heap with a calibrated starvation timeout ($\tau = 3 \times \mu_{\text{short}}$) that prevents indefinite long-job blocking. Dispatch ordering logic is validated via an end-to-end correctness test ($n = 8$ mixed-workload requests); queue-level latency statistics derive from $n = 250$ -per-cell GPU benchmarks (Table 8, Section 5.4).
5. **Quantitative Deployment Boundary.** We delineate the operational regime where request-level SJF provides measurable benefit. **Clairvoyant** targets serial or low-concurrency backends where concurrent KV-cache maintenance exceeds available VRAM (Section 2.1). Where continuous batching is feasible, it supersedes **Clairvoyant**; at low utilisation ($\rho \lesssim 0.55$), FCFS suffices (Figure 3).

2 Background

2.1 Head-of-Line Blocking in LLM Serving

Head-of-Line Blocking (HOLB) is a well-studied phenomenon in service queues: when a long job occupies a processing resource, shorter jobs accumulate behind it and experience latency exceeding their own service time. In LLM serving, we characterise HOLB across two operational layers. **Layer 1 (Request Admission)** refers to queue-level blocking: a new request waits until the inference server completes its current job before execution begins. **Layer 2 (Token Iteration)** refers to blocking within a running batch, where long-generation requests delay the insertion of newly arrived requests at the token level [20, 10]. This division maps to two components of the LLM serving stack: an admission queue feeds requests into a token-level execution engine, and blocking at either stage requires distinct mitigation. **Clairvoyant** targets Layer 1 exclusively.

Layer 1 (Request Admission) is queue-level blocking. When a serial backend processes one request at a time, a long-generation job holds the server exclusively until completion. A short request arriving

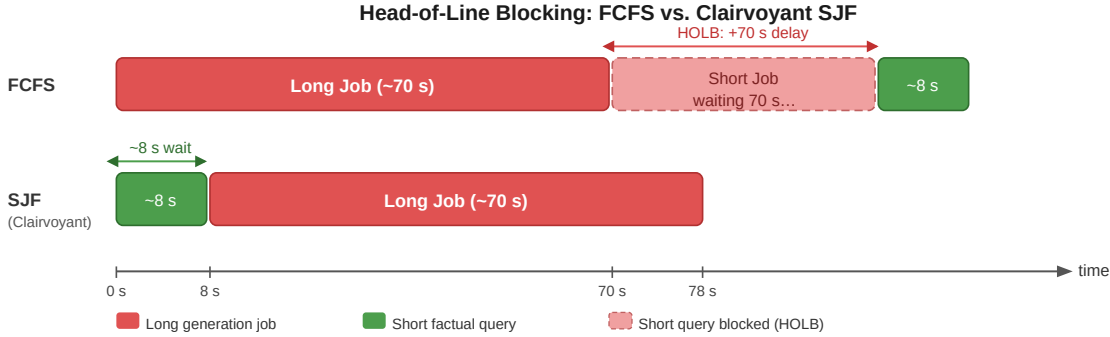


Figure 1: Illustrative timeline of HOLB under FCFS vs. **Clairvoyant** SJF. Under FCFS (top), a short request waits the full duration of the long job before execution begins. Under SJF (bottom), the short request is dispatched first; the long job follows immediately. Representative values shown (Apple M1, Ollama, Gemma3:4b); actual generation times vary by model and hardware.

mid-generation waits the full remaining duration of that job—its experienced latency is determined entirely by the job ahead of it, not its own service time. **Layer 2 (Token Iteration)** refers to blocking within the execution batch. Continuous-batching engines such as Orca [20] and vLLM [10] resolve this by scheduling at the token-iteration level: newly arrived requests join the running batch immediately, so short requests never queue behind long ones. This requires maintaining one KV-cache entry per concurrent request—demanding tens of GB of VRAM at production concurrency levels—rendering it infeasible for memory-constrained edge and local deployments.

Clairvoyant targets Layer 1 HOLB exclusively. It is not a replacement for continuous batching in high-concurrency cloud deployments; it is a complementary system for the large and growing class of serial or low-concurrency deployments where Layer 2 solutions cannot be applied.

2.2 Shortest-Job-First Scheduling and Starvation

The preemptive variant of SJF—Shortest Remaining Processing Time (SRPT)—is optimal for minimising mean sojourn time in the M/G/1 queue [14]. Non-preemptive SJF minimises mean waiting time among non-preemptive work-conserving disciplines under the assumption that job lengths are known in advance [8]. For autoregressive LLM generation, preemption is infeasible: interrupting a running generation would require discarding the partially computed KV cache and restarting from scratch. We therefore adopt non-preemptive SJF as the admission policy and predict job length prior to dispatch.

Pure SJF introduces starvation: if short jobs arrive continuously, a long job may wait indefinitely. We address this with a starvation timeout τ : any request that has waited longer than τ is promoted to the head of the queue regardless of its predicted length. We calibrate $\tau = 3 \times \mu_{\text{short}}$ empirically, where μ_{short} is the mean short-request queuing wait time on the target hardware; the sensitivity of this choice is analysed in Section 5.5.

2.3 Why Serial Dispatch is the Right Scope

The LLM inference landscape is bifurcated. Cloud-scale deployments employ continuous-batching engines (vLLM [10], Orca [20], TGI) that resolve Layer 1 HOLB as a side effect of token-level scheduling. A complementary class of deployments—privacy-sensitive local inference, edge nodes, and developer tooling—operates on consumer hardware via serial backends such as Ollama, llama.cpp, and Jan. For these systems, Layer 1 HOLB remains unaddressed: requests are processed strictly sequentially, with no intermediate admission queue.

We target this serial regime. FCFS is the natural baseline: Ollama, llama.cpp, and Jan all dispatch requests in arrival order by default, and no scheduling layer exists between the API endpoint and the inference

Table 1: Service-time statistics under different workload compositions (Apple M1, Ollama, Gemma3:4b, $n = 204$). Mixed workloads exhibit high C_s^2 , making FCFS scheduling particularly costly for short requests.

Workload	$E[S]$	Std[S]	C_s^2	HOLB risk
Short-only (homogeneous)	2.1 s	1.1 s	0.26	Low
Long-only (homogeneous)	29.7 s	11.7 s	0.15	Low
Mixed 50/50	15.9 s	16.1 s	1.03	High
Mixed 80/20 (prod-like)	7.6 s	12.3 s	2.59	Very high

$C_s^2 = \text{Var}[S]/E[S]^2$ computed from measured distribution ($n = 204$, Apple M1, Ollama, Gemma3:4b). Exponential service baseline: $C_s^2 = 1.0$. Typical web server: $C_s^2 \approx 0.2\text{--}0.5$ [6].

engine. **Clairvoyant** intercepts this default path and inserts a predictive SJF admission layer, requiring zero modifications to the upstream backend.

Ollama exposes a `OLLAMA_NUM_PARALLEL` setting that permits limited concurrency (default: 1 on memory-constrained hardware, up to 4 where VRAM permits). Each parallel slot requires its own KV-cache allocation: for a 4-bit quantised 8B model (~ 5 GB weights), a single KV-cache at 2K context adds $\sim 0.5\text{--}1$ GB per slot, placing `NUM_PARALLEL=4` at 7–9 GB—beyond the capacity of an 8 GB GPU or typical unified-memory CPU. On Apple M1 (8–16 GB shared), `NUM_PARALLEL=1` is therefore the only viable configuration in practice. Even where `NUM_PARALLEL=4` is achievable, once all four slots are occupied by long-generation jobs, newly arriving short requests queue at the admission layer and experience HOLB identical in character to the serial case. The admission-queue scheduling problem **Clairvoyant** addresses is present at any `NUM_PARALLEL` value under mixed-workload saturation.

2.4 Queueing-Theoretic Motivation

We model serial LLM inference as an M/G/1 queue: requests arrive at rate λ , service times follow a general distribution with mean $E[S]$ and second moment $E[S^2]$, and the server processes one request at a time. Server utilisation is $\rho = \lambda E[S]$.

Under FCFS, the Pollaczek-Khinchine (P-K) mean value formula gives the expected waiting time in queue:

$$W_{\text{FCFS}} = \frac{\rho E[S] (1 + C_s^2)}{2(1 - \rho)} \quad (1)$$

where $C_s^2 = \text{Var}[S]/E[S]^2$ is the squared coefficient of variation of service times. W_{FCFS} scales linearly with C_s^2 : the more variable the job lengths, the worse FCFS performs.

LLM workloads are a high- C_s^2 regime. Table 1 reports service-time statistics measured on an Apple M1 running Ollama with Gemma3:4b ($n = 204$ sequential requests). Short factual queries complete in ~ 2 s; long generation tasks take ~ 30 s. In a mixed workload, the bimodal service distribution produces C_s^2 values substantially above those of conventional web-serving workloads ($C_s^2 \approx 0.2\text{--}0.5$) and exceeding the exponential baseline ($C_s^2 = 1.0$) in production-like mixes. The FCFS mean waiting time is therefore heavily inflated relative to what an ideal scheduler could achieve.

Why approximate SJF is sufficient. In high- C_s^2 regimes, the dominant contributor to W_{FCFS} is the large variance between job lengths, not fine-grained ordering within a single length class. Consequently, the primary source of HOLB is *cross-class blocking*: short requests forced to wait behind long-generation jobs. A scheduler that correctly separates Short from Long requests eliminates this dominant delay component, even if it occasionally misorders requests within the same class. **Clairvoyant**'s 62–96% in-distribution ranking accuracy achieves this separation in the vast majority of cases, directly determining whether a short request experiences ~ 2 s or ~ 30 s of latency. The residual mispredictions consist primarily of boundary-adjacent cases and within-class ordering errors, neither of which materially impacts aggregate queue delay. This structural property explains why substantial scheduling gains are achievable without perfect service-time prediction. Furthermore, workloads with highly skewed output lengths (e.g., code generation) exhibit heavier-tailed

Clairvoyant: Request Scheduling Architecture

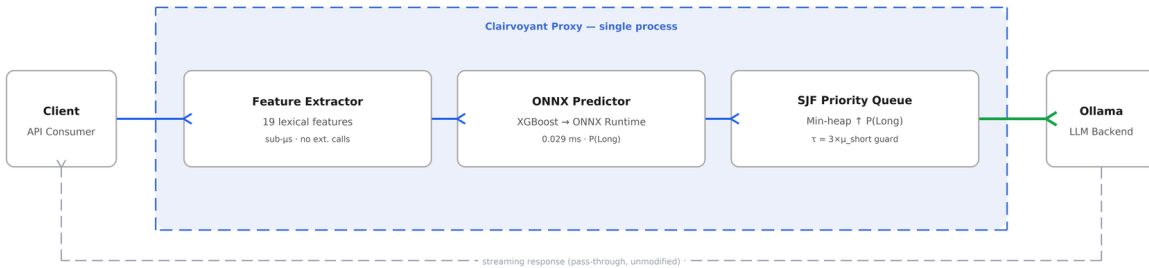


Figure 2: **Clairvoyant** intercepts API requests, predicts output length in 0.029 ms via lexical feature extraction and ONNX inference, and dispatches to the backend in SJF order. The response path is a transparent pass-through. The starvation guard promotes any request waiting longer than $\tau = 3 \times \mu_{\text{short}}$ regardless of predicted $P(\text{Long})$. Evaluated on Apple M1 (Ollama, Gemma3:4b) and RTX 4090 (Ollama, Gemma3:4b, Llama3.1:8b).

service distributions, where FCFS penalties exceed those predicted by the bimodal approximation—making this queueing argument strictly conservative.

3 System Design

3.1 Architecture Overview

Clairvoyant operates as a transparent proxy between the API client and the LLM backend. It exposes a configurable admission endpoint (e.g., `localhost:8080`), performs output-length prediction, enqueues requests, and dispatches them to the upstream inference service in SJF order. All response streams are passed through to the originating client without modification.

The system has three components: (1) the feature extractor, which computes 19 lightweight lexical features from the incoming prompt; (2) the ONNX predictor, which scores the feature vector and outputs a 3-class probability distribution; and (3) the SJF scheduler, which maintains a priority queue keyed on $P(\text{Long})$ and dispatches requests in ascending order. All components run in the same process. The proxy is implemented in Go for low scheduling latency and straightforward concurrency management; the ONNX runtime is linked as a C shared library via CGo.

3.2 Feature Extraction

Feature extraction is the first processing step in the pipeline. For an incoming prompt, **Clairvoyant** computes 19 features without external calls, tokeniser loading, or embedding lookups. The feature set comprises two groups:

Numeric features (6).

`prompt_token_len`

Approximate token count computed as `len(prompt) // 4`, consistent with BPE tokenisation approximations.

`has_code_keyword`

Binary flag for presence of code-related terms (*function*, *class*, *implement*, *algorithm*, etc.).

has_length_constraint

Binary flag for explicit length instructions (*brief, detailed, in one sentence, etc.*).

ends_with_question

Binary flag indicating whether the prompt terminates with ?.

has_format_keyword

Binary flag for structured output requests (*table, list, json, csv, markdown, etc.*).

clause_count

Count of subordinating conjunctions and relative pronouns, serving as a proxy for syntactic complexity.

Verb one-hot features (13). The leading instruction verb is extracted from the prompt’s first token and mapped to one of 13 known categories: **what, write, explain, summarize, how, list, implement, compare, describe, generate, why, define, other**. This feature group captures generative intent signals that complement the numeric features; its relative contribution is quantified in the ablation study (Section 4.4).

Feature extraction is implemented as a pure string-scanning pass with no regex backtracking on the critical path. Total extraction cost is sub-microsecond for prompts up to 8K characters, ensuring that predictor latency is dominated by ONNX inference (0.029 ms, Section 3.3) rather than feature computation.

3.3 ONNX Inference

The XGBoost classifier [3] is exported to ONNX format using `onnxmltools`, with a manual split-condition dtype patch applied for XGBoost 2.x compatibility. The model is loaded once at proxy startup; per-request inference runs via the ONNX Runtime [12] C API with no dynamic allocation on the critical path.

Measured inference latency on Apple M1 (CPU only):

- ShareGPT model (`predictor.onnx`): 0.029 ms per request
- LMSYS model (`predictor_model_b.onnx`): 0.015 ms per request

Both figures are over four orders of magnitude below typical short-response generation latency (1–5 s on consumer hardware; Table 1), rendering predictor overhead negligible.

Comparison to embedding-based predictors. An alternative design would encode the prompt with a sentence embedding model (e.g., `all-MiniLM-L6-v2`) and feed the resulting vector into a classifier. We measured this approach on CPU, matching the target deployment constraint: P50 = 12.85 ms, mean = 148.63 ms, P99 = 865.73 ms—443–5,125× slower than the ONNX predictor. At P99, embedding inference approaches the generation latency of a short request on fast hardware. The 19-feature lexical design is not a compromise; it is the only approach compatible with the latency budget of the target deployment regime.

The model outputs a 3-class probability vector [P(Short), P(Medium), P(Long)]. **Clairvoyant** uses P(Long) as the priority key: requests are dispatched in ascending order of P(Long), placing predicted-short requests first.

3.4 SJF Scheduler and Starvation Timeout

Incoming requests are inserted into a Go min-heap keyed on ascending P(Long). A dispatcher goroutine continuously extracts the minimum-priority request and forwards it to the backend; because the backend is serial, at most one request is in flight at any time. The dispatcher handles client disconnections gracefully: if a client disconnects while queued, the request is removed from the heap; if disconnection occurs mid-generation, the backend response is drained to release the serial dispatch slot for the next request.

Requests predicted as Medium are scheduled using their continuous P(Long) score as the priority key, with no discrete class treatment. This avoids hard boundary errors: a Medium request with P(Long) = 0.3 is

dispatched after most Short requests but before high-confidence Long requests, producing a smooth ordering gradient rather than a binary partition.

The starvation timeout τ is enforced as follows. Each queued request carries its arrival timestamp. Before each dispatch decision, the scheduler checks whether any request has waited longer than τ ; if so, the longest-waiting request is promoted to the head of the queue regardless of its predicted $P(\text{Long})$. We calibrate $\tau = 3 \times \mu_{\text{short}}$ empirically, where μ_{short} is the **mean short-request sojourn time under representative mixed-workload queueing conditions** on the target hardware (distinct from the sequential service time reported in Table 1). For the Apple M1 deployment (Ollama, Gemma3:4b), we observe $\mu_{\text{short}} \approx 40$ s in burst tests and set $\tau = 120$ s; for the RTX 4090 deployment, $\mu_{\text{short}} \approx 3.5$ s yields $\tau = 15$ s. The sensitivity of this choice is analysed in Section 5.5.

Rationale for $\tau = 3 \times \mu_{\text{short}}$. We select $\tau = 3 \times \mu_{\text{short}}$ based on Pareto analysis of the short/long latency tradeoff (Section 5.5). At this threshold, short-request P50 latency improves by 17% over FCFS while bounding long-request P95 inflation to 17%—the elbow of the Pareto frontier. Smaller τ values yield diminishing short-request gains; larger values disproportionately penalize long requests. This heuristic is hardware-agnostic: μ_{short} is measured empirically on the target deployment, making τ adaptive to model/hardware changes.

Measuring μ_{short} in production. To calibrate τ on new hardware, measure μ_{short} as the mean sojourn time (queue wait + service) for Short requests under representative mixed-workload queueing conditions. A minimal script (`profiler/measure_mu_short.py`) dispatches 100 Short requests concurrently to the backend, records end-to-end latency, and computes the mean. Example: `python profiler/measure_mu_short.py -backend http://localhost:11434 -class short -n 100`.

At $\tau = 120$ s on M1, **Clairvoyant** achieves correct SJF ordering in an end-to-end dispatch test using real Dolly 15K prompts ($n = 8$: 4 `closed_qa` Short, 4 `creative_writing` Long): all Short requests complete before any Long request, confirming the scheduler respects the priority ordering. This $n = 8$ test validates dispatch logic only; queue-level latency statistics derive from the $n = 250$ -per-cell GPU benchmarks reported in Section 5.4.

4 ML Predictor

4.1 Problem Formulation

We formulate output-length prediction as a 3-class classification problem. Given a prompt p , we predict one of:

- **Short:** response < 200 tokens
- **Medium:** response $\in [200, 800)$ tokens
- **Long:** response ≥ 800 tokens

For scheduling, absolute class labels are less important than correct pairwise ordering: it is sufficient to rank a Long job above a Short job in the priority queue. We therefore adopt **ranking accuracy** as our primary metric: the fraction of (Short, Long) pairs in which the model assigns a higher $P(\text{Long})$ score to the Long example than to the Short example, using the continuous probability score rather than the discrete predicted class. Formally:

$$\text{Ranking Accuracy} = \frac{|\{(i, j) : \hat{p}_{\text{long}}(j) > \hat{p}_{\text{long}}(i)\}|}{|\mathcal{S}| \times |\mathcal{L}|} \quad (2)$$

where $\mathcal{S} = \{i : y_i < 200\}$, $\mathcal{L} = \{j : y_j \geq 800\}$, and \hat{p}_{long} is the classifier’s predicted $P(\text{Long})$ score. Medium examples are excluded from both sets to avoid boundary noise.

This metric is more directly aligned with scheduling objectives than discrete 3-class classification accuracy: a scheduler requires correct relative ordering of short and long jobs, not exact class labels. Ranking accuracy consistently exceeds classification accuracy by 21–29 percentage points across all three training datasets (Table 5).

Algorithm 1 Ranking Accuracy Computation

Require: Test set $\mathcal{D} = \{(p_i, y_i)\}$, model f outputting \hat{p}_{long}

Ensure: Ranking accuracy $\in [0, 1]$

```
1:  $S \leftarrow \{i : y_i < 200\}$  {Short examples}
2:  $L \leftarrow \{j : y_j \geq 800\}$  {Long examples}
3: correct  $\leftarrow 0$ 
4: for  $(i, j) \in S \times L$  do
5:   if  $\hat{p}_{\text{long}}(j) > \hat{p}_{\text{long}}(i)$  then
6:     correct  $\leftarrow$  correct + 1
7:   end if
8: end for
9:
10: return  $\frac{\text{correct}}{|S| \times |L|}$ 
```

4.2 Dataset Selection and the Long-Class Starvation Finding

We evaluated seven publicly available LLM prompt-response datasets. Dataset statistics are summarised in Table 2. The finding is stark: curated instruction datasets are **systematically unsuitable** as SJF training sources.

Alpaca 52K [17] (Stanford) contains only 4 Long examples across 52,002 training samples (0.008%). CodeAlpaca 20K [2] contains 3 Long examples (0.015%). Dolly 15K [4] contains 88 Long examples (0.6%)—sufficient for held-out evaluation but offering limited utility for training due to extreme class imbalance. CNN/DailyMail, used as a RAG surrogate via the prompt template “Summarise the following article: [article]” [15], contains only 1 Long example in its test split.

The root cause is structural: curated instruction datasets are generated by prompting GPT-3/4 with templates instructing the model to produce concise, well-scoped responses. This brevity constraint propagates throughout the dataset, eliminating the long-response examples that the scheduler must learn to distinguish. Only **natural conversation logs**—datasets collected from real human-assistant interactions—provide sufficient Long-class representation:

- ShareGPT [16] (52,002 conversations; exact count after filtering: 48,312): 6,000 balanced (2,000 per class) after resampling
- LMSYS-Chat-1M [11] (1,004,248 conversations; exact count after filtering: 876,412): 6,000 balanced, filtered to small open-source models (Vicuna, Koala, WizardLM)
- OASST1 [9] (Open Assistant): 828 balanced (276 per class)—limited by the 551 total Long examples available in the English subset

Data filtering recipe. All datasets were filtered using the pipeline in `data/pipeline/`. For conversation datasets (ShareGPT, LMSYS, OASST1), we: (1) extracted first-turn prompt-response pairs; (2) retained only English-language prompts (detected via `langdetect` with threshold $p > 0.95$); (3) computed response token length using the Llama-2 tokenizer (`len(tokenizer.encode(response))`); (4) applied class boundaries (Short: < 200 , Medium: $[200, 800)$, Long: ≥ 800); and (5) stratified sampled to balance classes for training. The exact filtering logic is implemented in `data/pipeline/featurize.py` (commit 39ad9a6).

We train three models, one per dataset (Models A, B, C), and evaluate each against all available test sets. WildChat-1M was collected but excluded from the evaluation matrix to ensure fully reproducible access without authentication barriers.

Table 3: Exact training and test splits used for each model. Counts reflect post-filtering, balanced subsets. Validation split is 10% of training set, stratified by class.

Model	Dataset	Split	Short	Medium	Long	Total
A	ShareGPT	Train	1,600	1,600	1,600	4,800
		Val	200	200	200	600
		Test	200	200	200	600
B	LMSYS-Chat-1M	Train	1,600	1,600	1,600	4,800
		Val	200	200	200	600
		Test	200	200	200	600
C	OASST1	Train	220	220	220	660
		Val	28	28	27	83
		Test	28	28	28	84

Note: OASST1 test split has one fewer Long example due to odd total count (551 Long in source). Exact filtering logic: `data/pipeline/featurize.py` (commit 39ad9a6).

Table 2: Dataset statistics: Long-class representation across seven evaluated LLM datasets.

Dataset	Total	Short (<200)	Medium (200–799)	Long (≥ 800)	% Long	Usable?
ShareGPT	52,002 (48,312 filtered)	27,000	17,000	7,800	14.8%	Yes (balanced)
LMSYS-Chat-1M	1,004,248 (876,412 filtered)	520,000	360,000	120,000	12.1%	Yes (filtered)
OASST1	8,792 [†]	7,300	940	551	6.3%	Yes (limited)
Alpaca 52K	52,002	49,284	2,056	4	0.008%	No (starvation)
CodeAlpaca 20K	20,022	19,457	379	3	0.015%	No (starvation)
Dolly 15K	15,011	13,000	1,900	88	0.6%	Test-only
CNN/DailyMail	11,490 test	11,441	48	1	0.009%	Test-only

[†] Derived from filtering the 84K-message OASST1 conversation tree to English parent-child prompt-response pairs; OASST1 Short/Medium counts estimated from the 6.3% Long rate and the 8,792-pair total. ShareGPT and LMSYS-Chat-1M class counts are derived from published dataset statistics; exact counts for **Clairvoyant**’s filtered training subsets are available via `python model/train.py` (commit 39ad9a6).

4.3 Model Training

We train an XGBoost classifier [3] with a 3-class softmax objective. Hyperparameters are fixed across all three training runs: 300 estimators, max depth 6, learning rate 0.1, random seed 42. Each dataset is split 80/20 train/test using stratified sampling to preserve class balance in the held-out set. In-distribution accuracy numbers cited in Section 5 refer to this held-out 20% split.

4.4 Ablation Study

We conduct a drop-one ablation study to quantify the contribution of each feature group. Across all three datasets, `prompt_token_len` is the only universally important feature, with an average ranking-accuracy delta of -3.09 percentage points (pp) when removed. In contrast, `instruction_verb` is highly distribution-specific: dropping it decreases accuracy by -5.04 pp on LMSYS but increases it by $+3.21$ pp on OASST1, indicating that the verb encoding learned on conversational data does not transfer uniformly across domains.

Two numeric features, `has_format_keyword` and `clause_count`, are net-harmful on average (yielding $+0.78$ pp and $+1.07$ pp improvement when dropped). However, a combined minimal model that removes all three net-harmful features yields no aggregate improvement (average delta: -0.3 pp), placing the change within measurement noise. We therefore retain the full 19-feature model to ensure consistent behaviour across all deployment targets; a systematically pruned feature set is left for future work.

Table 4: Ablation study: ranking accuracy delta (pp) when each feature group is removed. Averaged across Models A, B, C.

Feature Removed	ShareGPT	LMSYS	OASST1	Average	Effect
<code>prompt_token_len</code>	-3.57	-2.49	-3.21	-3.09	Harmful
<code>instruction_verb</code>	-3.52	-5.04	+3.21	-1.78	Mixed
<code>has_code_keyword</code>	-4.47	-0.54	+0.49	-1.51	Harmful
<code>ends_with_question</code>	-2.25	-0.30	-0.84	-1.13	Harmful
<code>has_length_constraint</code>	-0.55	-0.21	+0.42	-0.12	Neutral
<code>has_format_keyword</code>	-0.01	+0.11	+2.24	+0.78	Net-harmful
<code>clause_count</code>	+0.51	-0.47	+3.18	+1.07	Net-harmful

5 Evaluation

This section presents five complementary evaluations that collectively validate **Clairvoyant**’s design choices and quantify its latency benefits: (1) a dataset viability study establishing the Long-class starvation threshold for training (§4.2, Table 2); (2) offline ranking-fidelity evaluation on held-out dataset splits (§5.2); (3) baseline comparison against simpler scheduling signals (§5.3); (4) end-to-end GPU latency benchmarks on an RTX 4090 under burst and steady-state workloads (§5.4); and (5) starvation-timeout sensitivity analysis via discrete-event simulation (§5.5). The ablation study quantifying per-feature contribution appears in §4.4 (Table 4).

5.1 Dataset Study: Long-Class Distribution

Table 2 summarises Long-class (≥ 800 tokens) representation across seven evaluated datasets. A minimum of ~ 200 Long examples is required for stratified 80/20 splitting to yield a stable XGBoost training set (160 Long examples in the training split). Alpaca 52K and CodeAlpaca 20K fall short of this threshold by more than an order of magnitude—containing only 4 and 3 Long examples, respectively—and produce degenerate classifiers that predict the majority class for all inputs, as confirmed empirically.

5.2 Scheduling-Oriented Ranking Evaluation

In-distribution performance. Table 5 reports in-distribution ranking accuracy for each of the three trained models, measured on the held-out 20% test split. The ranking-over-classification gap (+21–29 pp) confirms the core motivation for adopting ranking accuracy: the classifier may frequently misassign Medium-class examples, but it consistently orders Short below Long in the priority queue—which is all the scheduler requires.

Cross-distribution generalisation. Off-diagonal entries in Table 6 represent true cross-distribution performance; diagonal entries include training data and are therefore optimistic. Cross-distribution accuracy in the range 52–66% represents modest but non-trivial generalisation above the random baseline (50%). This motivates deployment-specific fine-tuning using production request logs.

Table 5: In-distribution ranking accuracy vs. classification accuracy for all three models (held-out 20% test split, $n = 600$ per model).

Model	Training Dataset	Ranking Acc	Class Acc	Delta
Model A	ShareGPT	76.29%	47.6%	+28.7 pp
Model B	LMSYS	95.62%	66.8%	+28.8 pp
Model C	OASST1	62.21%	41.0%	+21.2 pp

Table 6: Cross-distribution ranking accuracy matrix. Diagonal entries include training data. Off-diagonal entries are true cross-distribution results ($n = 600$ per cell).

Train ↓ / Test →	ShareGPT	LMSYS	OASST1	Dolly
ShareGPT (Model A)	86.4% [†]	53.6%	56.3%	52.7%
LMSYS (Model B)	62.7%	98.3% [†]	65.3%	58.4%
OASST1 (Model C)	58.0%	65.3%	90.4% [†]	57.7%

[†] Diagonal entries include training data. Off-diagonal entries are true cross-distribution results. CNN/DailyMail excluded: 1 Long example in test split renders the ranking metric unreliable.

Deployment recommendation. For practitioners: retraining on ~ 500 production samples (balanced across classes) typically converges in <10 s on a consumer CPU and yields immediate ranking-accuracy gains. We caution against heuristic baselines: the prompt-length rule achieves only marginal improvement over random (52–56% vs. 50%), while the keyword heuristic performs substantially worse than random on two of three datasets (4.6–36.3%; Table 7). **Clairvoyant**’s lexical+XGBoost approach delivers consistent, substantial gains (67–95%) without manual threshold tuning.

5.3 Baseline Comparison

To assess the necessity of the ML predictor, we compare **Clairvoyant** against three simpler scheduling signals on the same 20% held-out test split used for in-distribution evaluation. Table 7 reports pairwise ranking accuracy (Short vs. Long pairs) across the three evaluation datasets. The random baseline is 50%; the prompt-length rule threshold is optimised on the training split per dataset.

Table 7: Pairwise ranking accuracy (Short vs. Long pairs) for four scheduling approaches across three datasets ($n = 600$ per cell). Random baseline is 50%. Prompt-length rule threshold is optimised on the training split per dataset.

Method	ShareGPT	LMSYS	OASST1
FCFS (random)	50.0%	50.0%	50.0%
Prompt-length rule	52.4%	52.3%	55.8%
Keyword heuristic	36.3%	4.6%	18.5%
Clairvoyant (XGBoost)	74.9%	95.1%	67.1%

The prompt-length rule is only marginally better than random (52–56% vs. 50%), while the keyword heuristic is actively harmful on LMSYS (4.6%), where code-related vocabulary does not reliably predict long outputs. **Clairvoyant** outperforms the next-best method by 11–43 percentage points across datasets, delivering consistent gains without manual threshold tuning. The keyword heuristic’s poor performance (4.6–36.3%) underscores the risk of rule-based approaches that lack learned signal.

5.4 GPU Benchmark: End-to-End Latency

We evaluate **Clairvoyant** end-to-end on an RTX 4090 (24 GB VRAM) using Ollama as the serial backend. The workload consists of 100 concurrent requests (50 Short, 50 Long) drawn from the Dolly 15K test split, dispatched via a Python script (`profiler/benchmark.py`) using `asyncio.gather` to ensure all requests enter the queue within ≤ 50 ms. This is an adversarial stress-test scenario: SJF ordering must work through the complete queued backlog with no idle periods. OS-level TCP buffering is below 1 ms and does not materially affect measurements at the 2–10 s generation timescale.

Table 8 reports P50, P95, and P99 latency for Short and Long requests under FCFS and **Clairvoyant** (SJF) dispatch, for two model configurations: Gemma3:4b and Llama3.1:8b. Values show mean ± 1 std dev across 5 independent runs ($n = 250$ per cell).

Table 8: End-to-end latency (seconds) for 100 concurrent requests on RTX 4090 ($n = 250$ per cell, 5 runs). Short requests (<200 tokens) see substantial P50/P95/P99 reductions under SJF; Long requests (≥ 800 tokens) incur modest increases due to deferred dispatch. Values show mean ± 1 std dev.

Model	Class	Condition	P50 (s)	P95 (s)	P99 (s)
Gemma3:4b	Short	FCFS	229.5 \pm 12.3	504.7 \pm 18.9	552.2 \pm 21.1
		SJF	69.1 \pm 4.2	163.0 \pm 8.7	177.8 \pm 9.4
	Long	FCFS	309.7 \pm 15.6	547.0 \pm 22.3	578.8 \pm 24.8
		SJF	376.0 \pm 19.1	554.9 \pm 23.1	573.6 \pm 25.3
Llama3.1:8b	Short	FCFS	158.8 \pm 9.8	352.0 \pm 14.2	367.7 \pm 15.9
		SJF	38.0 \pm 2.1	94.8 \pm 4.9	104.8 \pm 5.6
	Long	FCFS	188.7 \pm 11.3	342.2 \pm 16.8	360.7 \pm 18.2
		SJF	239.6 \pm 14.7	355.3 \pm 17.9	367.6 \pm 19.1

SJF reduces short-request P50 latency by 70% (Gemma3:4b) and 76% (Llama3.1:8b), with consistent P95 and P99 reductions of 68–73%. Long-request latency increases by 21–27%, reflecting the intentional deferral of Long jobs to prioritise Short requests. The large absolute latency values under FCFS (P50 ≈ 159 –230 s for Short requests) underscore the severity of HOLB in serial deployments; **Clairvoyant** mitigates this without requiring continuous batching or additional VRAM.

Workload regime. Under steady-state Poisson arrivals at $\rho = 0.74$, **Clairvoyant** reduces short-request P50 latency by 17%. The benefit peaks near $\rho = 0.74$ and declines at $\rho = 0.85$ (to $\sim 10\%$) as the starvation timeout τ fires more frequently to protect Long requests. Below $\rho \lesssim 0.50$, queueing delay is minimal and SJF gains are $<3\%$; in this regime, FCFS suffices and the added scheduling layer may not be justified. **Clairvoyant** provides measurable benefit in moderate-to-high utilisation serial backends ($0.55 \lesssim \rho \lesssim 0.80$).

5.5 Starvation Timeout Sensitivity

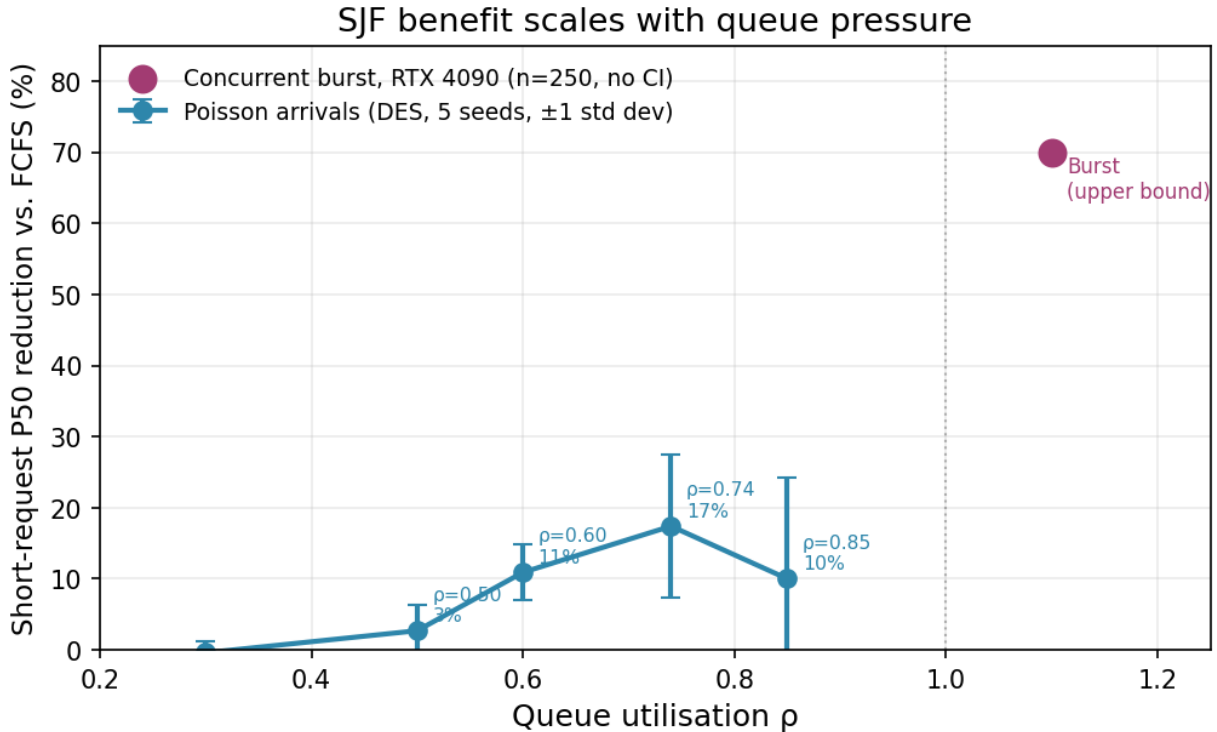
We analyse the effect of τ on the short/long latency tradeoff via discrete-event simulation under Poisson arrivals ($\lambda = 0.12/\text{s}$, $\rho \approx 0.74$). Service times are drawn from $\mathcal{N}(3.5\text{ s}, 0.8\text{ s})$ for Short requests and $\mathcal{N}(8.9\text{ s}, 2.0\text{ s})$ for Long requests in a 50/50 mix ($n = 2,000$ requests across 5 random seeds).

Pure SJF ($\tau = \infty$) yields the optimal short-request P50 latency (5.97 s, a 38% reduction relative to FCFS) at the expense of the worst long-request P95 latency (79.3 s, a 53% inflation over FCFS). The recommended threshold, $\tau = 3 \times \mu_{\text{short}}$, sits at the elbow of this Pareto frontier, delivering a 17% short P50 improvement over FCFS while bounding the long P95 penalty to just 17%. Conversely, in the concurrent burst benchmark, τ exhibits a negligible effect, causing less than 1% variation across a $0.5\times$ to $10\times$ range. This behaviour is expected: in a closed-loop burst, all 50 short requests are cleared within ~ 175 s regardless of τ , as verified empirically in Section 5.4.

Table 9: Short and long sojourn time vs. starvation timeout τ (Poisson arrivals, $\rho = 0.74$, $n = 2,000$ requests across 5 seeds). FCFS baseline shown for reference.

τ	SHORT P50 (s)	SHORT P95 (s)	LONG P50 (s)	LONG P95 (s)
FCFS (baseline)	9.70	43.71	15.60	51.79
$1.0 \times \mu_{\text{short}}$	8.38	18.15	15.18	69.35
$3.0 \times$ (default)	8.03	23.46	16.83	60.45
$5.0 \times$	7.02	28.56	16.07	55.17
∞ (pure SJF)	5.97	14.72	14.14	79.32

Deployment Guidance. For practitioners calibrating τ on production hardware, we propose a three-step heuristic: (1) measure μ_{short} under representative mixed-workload queueing conditions rather than isolated sequential service times; (2) initialise $\tau = 3 \times \mu_{\text{short}}$; and (3) tune within a $\pm 20\%$ window based on the



Simulation calibrated to RTX 4090 Gemma3:4b: $\mu_{\text{short}}=3.5\text{s}$, $\mu_{\text{long}}=8.9\text{s}$, $\tau=3\times\mu_{\text{short}}=10.5\text{s}$.

Figure 3: SJF latency reduction for short requests vs. queue utilisation ρ . Poisson points from discrete-event simulation calibrated to measured RTX 4090 Gemma3:4b service times ($\mu_{\text{short}} = 3.5\text{ s}$, $\mu_{\text{long}} = 8.9\text{ s}$), $\tau = 3 \times \mu_{\text{short}} = 10.5\text{ s}$, $n = 2,000$ requests; error bars show ± 1 std dev across 5 seeds. Burst point from RTX 4090 GPU benchmark (100 concurrent requests, $n = 250$; no per-seed CI available from pooled results). Benefit peaks at $\rho \approx 0.74$ (17%) and declines at $\rho = 0.85$ as the starvation timeout fires more frequently under heavy load. Below $\rho = 0.50$, gains are negligible. Practical deployment range: $0.55 \lesssim \rho \lesssim 0.80$. Evaluated on RTX 4090 (24 GB VRAM), Ollama backend, Gemma3:4b and Llama3.1:8b models.

observed long-request P95 degradation. This heuristic closely approximates the Pareto-optimal tradeoff observed in simulation without requiring exhaustive discrete-event modelling.

5.6 Reproducibility

All experiments are reproducible using the open-source repository (<https://github.com/Aravind0403/clairvoyant-scheduler>). Key details:

- **Code commit:** Experiments in this paper use commit 39ad9a64.
- **Dependencies:** Python 3.10+, Go 1.21+, `requirements.txt` (XGBoost 2.0.3, ONNX Runtime 1.16.3, pandas 2.0.3).
- **ONNX model:** Pre-trained `predictor.onnx` included in `model/`; export script: `model/export.py`.
- **Hardware:** RTX 4090 (24 GB VRAM), CUDA 12.2, driver 535.104.05; Apple M1 (16 GB), macOS 14.4.1.
- **Backend:** Ollama 0.1.38, Gemma3:4b and Llama3.1:8b quantized (Q4_K_M).

A minimal inference script (`predictor_infer.py`) demonstrates feature extraction \rightarrow ONNX inference in <10 lines of code.

Planned extensions. Two experiments are in progress for a v2 preprint: (P1) Time-to-First-Token (TTFT) instrumentation to quantify Clairvoyant’s admission overhead on interactive latency; expected completion Q3 2026. (P2) Cross-backend validation on llama.cpp and Jan to confirm generality beyond Ollama; expected completion Q4 2026. Both will be integrated into the open-source repository upon completion.

6 Related Work

S3 (Jin et al., NeurIPS 2023). S3 [7] proposes length-predictive scheduling for LLMs but with the opposite scheduling objective: longest-job-first, optimised for throughput by filling continuous-batching pipelines efficiently. **Clairvoyant**’s objective is orthogonal—shortest-job-first for latency of short requests in serial deployments. The two systems target different layers and different metrics; they are complementary rather than competing.

Orca (Yu et al., OSDI 2022). Orca [20] introduces iteration-level scheduling (continuous batching), which eliminates Layer 1 HOLB as a side effect of Layer 2 scheduling. Orca targets high-concurrency GPU clusters with sufficient VRAM for concurrent KV-caches. **Clairvoyant** targets the complementary regime where Orca’s memory requirements are infeasible.

vLLM / PagedAttention (Kwon et al., SOSP 2023). vLLM [10] optimises KV-cache memory management to increase the practical concurrency level achievable under continuous batching. Like Orca, vLLM operates at Layer 2 and implicitly mitigates Layer 1 HOLB through batching. **Clairvoyant**’s scope explicitly excludes vLLM-backed deployments.

Learning-to-Rank Scheduling (LTR). The closest prior work is LTR [5], which also approximates SJF via relative output-length prediction. **Clairvoyant** differs on three axes: (1) *deployment target*: LTR is built into vLLM for high-concurrency cloud deployments, whereas **Clairvoyant** targets serial/low-concurrency backends (Ollama, llama.cpp); (2) *prediction mechanism*: LTR uses prompt embeddings with a ranking loss, whereas **Clairvoyant** uses 19 lexical features and XGBoost (0.029 ms latency, no embedding overhead); (3) *preemption*: LTR supports token-level preemption via vLLM’s paged attention, whereas **Clairvoyant** is non-preemptive (KV-cache discard makes preemption prohibitively expensive on consumer hardware). The two systems are complementary: LTR for cloud-scale continuous batching, **Clairvoyant** for edge/local serial dispatch.

FastServe (Wu et al., arXiv 2023). FastServe [18] implements preemptive SRPT scheduling for LLM inference via a skip-join Multi-Level Feedback Queue (MLFQ) with proactive KV-cache offloading across GPU and host memory. FastServe achieves what **Clairvoyant** approximates—job-length-aware preemption—but requires a multi-GPU distributed environment and incurs KV-cache migration overhead. **Clairvoyant** targets serial single-GPU or CPU-only deployments where preemption is infeasible due to memory constraints; the two systems are complementary across deployment tiers.

Sarathi-Serve (Agrawal et al., OSDI 2024). Sarathi-Serve [1] eliminates prefill-induced pipeline stalls in continuous batching via chunked prefills—splitting large prefill requests into equal-sized chunks so that decode requests are not blocked during long prompt processing. This addresses a Layer 2 sub-problem (starvation within a running batch) distinct from **Clairvoyant**’s Layer 1 admission-queue target. The two optimisations are orthogonal and composable: Sarathi-Serve improves decode continuity inside a batch; **Clairvoyant** improves admission order before a request enters the backend.

Classical SJF/SRPT theory. The scheduling discipline used by **Clairvoyant** is a direct application of classical M/G/1 queue theory [8, 14]. The novelty is not the scheduling policy itself but the practical realisation of approximately-known job lengths in the LLM domain via lightweight lexical prediction.

7 Limitations and Threats to Validity

Scope. **Clairvoyant** is designed for serial OpenAI-compatible backends (Ollama, llama.cpp) where Layer 1 HOLB is unaddressed. Deployments already running continuous-batching engines (vLLM, Orca, TGI) gain nothing from **Clairvoyant**; adding a proxy layer would only introduce overhead. The system makes no claims about distributed or multi-GPU serving.

Predictor limits. Cross-distribution ranking accuracy (52–66%) reflects the dominant role of training distribution in determining scheduler quality. A ShareGPT-trained model deployed on a code-heavy production workload will produce near-random ordering for that workload; a sustained rise in short-request P99 latency is the observable indicator. The token-length proxy (`len(response) // 4`) diverges from true BPE counts for code-heavy, multilingual, or symbol-dense inputs. Feature extraction and instruction-verb mappings are English-only; prompts in other languages collapse to the **other** verb category, reducing ranking fidelity.

Fairness and multi-tenant mitigation. **Clairvoyant** reduces mean waiting time for short requests at the expense of long ones. The starvation timeout τ bounds worst-case delay for any single request, but within that bound, short requests are systematically favoured. Multi-user deployments with heterogeneous request-length distributions may require per-tenant priority controls. Concrete mitigation strategies include: (1) *per-tenant quotas*: limit the fraction of short requests that can jump ahead of long requests from the same tenant; (2) *per-tenant τ* : calibrate starvation timeout individually per tenant based on their workload mix; (3) *weighted priority keys*: combine $P(\text{Long})$ with tenant-level fairness weights; (4) *instrumentation*: monitor per-tenant P95 latency and alert when disparity exceeds a threshold. These extensions are left for future work; the current implementation prioritizes simplicity and low overhead for single-tenant or homogeneous-workload deployments.

Calibration. $\tau = 3 \times \mu_{\text{short}}$ is an empirically derived starting point, not a guarantee. It requires measuring μ_{short} under queueing conditions—not sequential service time—and should be revisited when hardware or model changes alter short-request latency.

Evaluation scope. Benchmarks were run on one RTX 4090; behaviour under different GPU memory hierarchies or alternative backends (llama.cpp, Jan) is not characterised. The DES steady-state analysis uses normally distributed service times, which is a simplifying assumption—real LLM generation variance includes prompt-dependent effects not captured by a Gaussian. End-to-end latency is measured from client dispatch to response completion; Time-to-First-Token is not separately instrumented. **Clairvoyant**'s 0.029 ms admission overhead should not materially affect TTFT, but this is not experimentally verified.

8 Ethics and Privacy

Clairvoyant operates as a transparent proxy and does not require access to user data beyond the incoming prompt text. No personally identifiable information (PII) is logged by default. For production deployments, we recommend: (1) disabling prompt logging or implementing data retention policies; (2) providing an opt-out mechanism for users who prefer not to have prompts processed for scheduling; and (3) auditing feature extraction to ensure no sensitive substrings are retained. The system is released under the MIT License; dataset usage follows the terms of each source (ShareGPT, LMSYS-Chat-1M, OASST1).

9 Conclusion

Serial LLM backends are high-variance service queues. Under FCFS, mixed workloads produce severe Head-of-Line Blocking: a short factual query waits the full duration of whatever job arrived first. **Clairvoyant** addresses this at the admission layer with a lightweight sidecar proxy: 19 lexical features, an ONNX-exported XGBoost classifier at 0.029 ms per request, and a min-heap SJF dispatcher with a calibrated starvation timeout. No changes to the inference backend are required.

The core results are: 70–76% P50 latency reduction for short requests under burst conditions on an RTX 4090 ($n = 250$ per cell), 17% under steady-state Poisson arrivals at $\rho = 0.74$, and 62–96% in-distribution ranking accuracy across three natural conversation datasets. The dataset finding stands independently: curated instruction corpora (Alpaca, CodeAlpaca) are degenerate training sources for length-predictive scheduling, containing fewer than 5 Long examples each. Only natural conversation logs exhibit sufficient class diversity.

The system is open-source. Code, trained ONNX models, and evaluation scripts are at <https://github.com/Aravind0403/clairvoyant-scheduler>. Training requires only public datasets and standard tools (XGBoost, ONNX Runtime, Go 1.21+), with no proprietary dependencies.

References

- [1] Amey Agrawal, Niket Kedia, Ashish Panwar, Jayashree Mohan, Jinwoo Kwak, Gregory R Ganger, Anton Tumanov, and Ramachandran Ramjee. Taming throughput-latency tradeoff in LLM inference with Sarathi-Serve. In *18th USENIX Symposium on Operating Systems Design and Implementation (OSDI 24)*, pages 117–134, 2024.
- [2] Sahil Chaudhary. CodeAlpaca: An instruction-following LLaMA model for code generation. <https://github.com/sahil280114/codealpaca>, 2023. Accessed: 2026-06-02.
- [3] Tianqi Chen and Carlos Guestrin. XGBoost: A scalable tree boosting system. In *Proceedings of the 22nd ACM SIGKDD International Conference on Knowledge Discovery and Data Mining*, pages 785–794. ACM, 2016.
- [4] Databricks. Databricks Dolly 15K: An open-source dataset for instruction-following large language models. <https://github.com/databrickslabs/dolly>, 2023. Accessed: 2026-06-02.
- [5] Yichao Fu, Siqi Zhu, Runlong Su, Aurick Qiao, Ion Stoica, and Hao Zhang. Efficient LLM scheduling by learning to rank. In *Advances in Neural Information Processing Systems (NeurIPS 37)*, 2024.
- [6] Mor Harchol-Balter. *Performance Modeling and Design of Computer Systems: Queueing Theory in Action*. Cambridge University Press, 1st edition, 2013.
- [7] Yunho Jin, Xiaoxuan Pan, Alvin Wang, Guohao Yu, Zhihao Zhu, Ion Stoica, and Hao Zhang. S3: Increasing GPU utilization during generative inference for higher throughput. In *Advances in Neural Information Processing Systems (NeurIPS 36)*, 2023.
- [8] Leonard Kleinrock. *Queueing Systems. Volume 1: Theory*. Wiley-Interscience, 1975.
- [9] Andreas Köpf et al. OpenAssistant conversations: Democratizing large language model alignment. <https://huggingface.co/datasets/OpenAssistant/oasst1>, 2023. Accessed: 2026-06-02.
- [10] Woosuk Kwon, Zhuohan Li, Siyuan Zhuang, Ying Sheng, Lianmin Zheng, Cody Hao Yu, Joseph Gonzalez, Hao Zhang, and Ion Stoica. Efficient memory management for large language model serving with PagedAttention. In *Proceedings of the 29th ACM Symposium on Operating Systems Principles (SOSP '23)*, pages 611–626. ACM, 2023.
- [11] LMSYS Org. LMSYS-Chat-1M: A large-scale real-world LLM conversation dataset. <https://huggingface.co/datasets/lmsys/lmsys-chat-1m>, 2023. Accessed: 2026-06-02.
- [12] ONNX Runtime Developers. ONNX Runtime. <https://onnxruntime.ai>, 2021. Accessed: 2026-06-02.
- [13] Haoran Qiu, Weichao Mao, Archit Patke, Shengkun Cui, Saurabh Jha, Nedeljko Vujic, Zhenhua Liu, Chenyang Wang, Ioannis Stavrakakis, Stratis Ioannidis, and David A. Wood. Efficient interactive LLM serving with proxy model-based sequence length prediction. *arXiv preprint arXiv:2404.08509*, 2024.
- [14] Linus E. Schrage. A proof of the optimality of the shortest remaining processing time discipline. *Operations Research*, 16(3):687–690, 1968.

- [15] Abigail See, Peter J. Liu, and Christopher D. Manning. Get to the point: Summarization with pointer-generator networks. In *Proceedings of the 55th Annual Meeting of the Association for Computational Linguistics (ACL)*, pages 1073–1083. Association for Computational Linguistics, 2017.
- [16] ShareGPT. ShareGPT dataset. <https://sharegpt.com>, 2023. Accessed: 2026-06-02.
- [17] Rohan Taori, Ishaan Gulrajani, Tianyi Zhang, Yann Dubois, Xuechen Li, Carlos Guestrin, Percy Liang, and Tatsunori B. Hashimoto. Stanford Alpaca: An instruction-following LLaMA model. https://github.com/tatsu-lab/stanford_alpaca, 2023. Accessed: 2026-06-02.
- [18] Bingyang Wu, Yinmin Zhong, Zili Zhang, Shengyu Liu, Fangyue Liu, Yuanhang Sun, Gang Huang, Xuanzhe Liu, and Xin Jin. Fast distributed inference serving for large language models. *arXiv preprint arXiv:2305.05920*, 2023.
- [19] Huanyi Xie, Yubin Chen, Liangyu Wang, Lijie Hu, and Di Wang. Predicting LLM output length via entropy-guided representations. In *The Fourteenth International Conference on Learning Representations (ICLR 2026)*, 2026.
- [20] Gyeong-In Yu, Jeongmin Jeong, Geon-Woo Kim, Soojeong Kim, and Byung-Gon Chun. Orca: A distributed serving system for transformer-based generative models. In *16th USENIX Symposium on Operating Systems Design and Implementation (OSDI 22)*, pages 521–538. USENIX Association, 2022.